J. Cent. South Univ. (2015) 22: 4856−4863
DOI: 10.1007/s11771-015-3037-1

Springer

Unsteady boundary layer flow and heat transfer over an exponentially shrinking sheet with suction in a copper-water nanofluid

Aurang Zaib[1], Krishnendu Bhattacharyya[2], Sharidan Shafie[3]

1. Department of Mathematical Sciences, Federal Urdu University of Arts, Science & Technology, Gulshan-e-Iqbal Karachi, Pakistan;
2. Department of Mathematics, The University of Burdwan, Burdwan 713104, West Bengal, India;
3. Department of Mathematical Sciences, Faculty of Science, Universiti Teknologi Malaysia, Johor Bahru, 81310, Skudai, Johor, Malaysia

Abstract: An analysis of unsteady boundary layer flow and heat transfer over an exponentially shrinking porous sheet filled with a copper-water nanofluid is presented. Water is treated as a base fluid. In the investigation, non-uniform mass suction through the porous sheet is considered. Using Keller-box method the transformed equations are solved numerically. The results of skin friction coefficient, the local Nusselt number as well as the velocity and temperature profiles are presented for different flow parameters. The results showed that the dual non-similar solutions exist only when certain amount of mass suction is applied through the porous sheet for various unsteady parameters and nanoparticle volume fractions. The ranges of suction where dual non-similar solution exists, become larger when values of unsteady parameter as well as nanoparticle volume fraction increase. So, due to unsteadiness of flow dynamics and the presence of nanoparticles in flow field, the requirement of mass suction for existence of solution of boundary layer flow past an exponentially shrinking sheet is less. Furthermore, the velocity boundary layer thickness decreases and thermal boundary layer thickness increases with increasing of nanoparticle volume fraction in both non-similar solutions. Whereas, for stronger mass suction, the velocity boundary layer thickness becomes thinner for the first solution and the effect is opposite in the case of second solution. The temperature inside the boundary layer increases with nanoparticle volume fraction and decreases with mass suction. So, for the unsteadiness and for the presence of nanoparticles, the flow separation is delayed to some extent.

Key words: unsteady boundary layer; heat transfer; nanofluid; exponentially shrinking sheet; dual non-similar solutions

1 Introduction

The study on heat transfer in the flow over a stretching/shrinking sheet is very significant in recent years. The development of this area of research is stimulated by the presence of a variety of real world applications in many industrial and engineering processes. Extrusion, paper production, glass blowing, hot rolling, artificial fibers and extraction of polymer are examples of such applications. The qualities of the final products depend to a great extent on the rate of cooling. So, to get better product the heat transfer should be controlled. CRANE [1] first reported the exact solution of the boundary layer flow over a stretching sheet. On the other hand, the flow over a shrinking sheet was first studied by WANG [2]. Later, MIKLAVČIČ and WANG [3] established the existence and uniqueness of the similarity solution of the equation for the steady flow due to a shrinking sheet. The boundary layer flow near a stagnation-point towards a shrinking sheet was considered by WANG [4]. As reported by MIKLAVČIČ and WANG [3] and WANG [4], the flow over a shrinking sheet is likely existing in the case of suction or considering a stagnation point. Since then many researchers are considering the flow over a shrinking sheet in many physical aspects. The power law velocity of the shrinking sheet was considered by FANG [5] and the dual solutions were obtained subject to wall mass transfer. BHATTACHARYYA [6] investigated MHD boundary layer flow and heat transfer over a shrinking sheet in the presence of heat source/sink and mass suction. HAYAT et al [7] studied MHD boundary layer flow near a stagnation point towards a heated shrinking surface in the presence of heat generation/absorption. BHATTACHARYYA et al [8] investigated the MHD boundary layer stagnation-point flow and mass transfer over a permeable shrinking sheet in the presence of

Received date: 2014−11−07; **Accepted date:** 2015−02−11
Corresponding author: Krishnendu Bhattacharyya, PhD; Tel: +919−474634200; E-mail: krish.math@yahoo.com; krishnendu.math@gmail.com

suction/blowing and chemical reaction. The boundary layer flow with heat transfer near a stagnation point over a shrinking sheet with non-uniform heat flux was considered by BHATTACHARYYA [9]. MIDYA [10] examined the MHD boundary layer flow and heat transfer towards a shrinking sheet in the presence of radiation and heat sink. MAGYARI and KELLER [11] studied the boundary layer flow and heat transfer over an exponentially stretching sheet. The steady two-dimensional boundary layer flow and heat transfer over an exponential shrinking sheet subjected to the suction was considered by BHATTACHARYYA [12] and the magnetic effect on the flow was reported by BHATTACHARYYA and POP [13]. BHATTACHARYYA and VAJRAVELU [14] explored some important characteristics of the stagnation-point flow and heat transfer over an exponentially shrinking sheet. On the other hand, the unsteady boundary layer flow over a shrinking sheet with suction was examined by FANG et al [15]. CORTELL [16] considered the two-dimensional and axisymmetric MHD boundary layer viscous flow induced by a shrinking sheet with suction. Recently, BHATTACHARYYA [17] discussed the unsteady boundary layer and heat transfer near a stagnation-point towards a shrinking/stretching sheet.

Considerable efforts have been directed towards the study on nanofluid due to its numerous industrial applications, such as in nanodrug delivery, thermal therapy for cancer treatment, power generation, heating and cooling processes, and chemical processes. Most of the common heat transfer fluids, such as mineral oil, water, and ethylene glycol, have a limitation in heat transfer process because of their low heat transfer properties. One of the best techniques to increase the thermal conductivity of these fluids is by suspending the solid nanoparticles into the base fluids, i.e., by making it nanofluid, and consequently, the heat transfer performance of fluid becomes excellent. The word “nanofluid” was proposed by CHOI [18], referring to dispersions of nanoparticles in the common fluids. In recent times, many investigations regarding nanofluids have been reported [19−22]. MANKINDE and AZIZ [23] studied the boundary layer flow immersed in a nanofluid over a linearly stretching surface. The boundary layer flow of a nanofluid near a stagnation-point towards a linear stretching surface was discussed by MUSTAFA et al [24]. RANA and BHARGAVA [25] investigated steady boundary layer flow filled with nanofluid over a nonlinear stretching surface. Whereas, HADY et al [26] showed the heat transfer analysis of a nanofluid over a nonlinear stretching sheet with thermal radiation and variable wall temperature. NADEEM and LEE [27] examined the boundary layer flow immersed in a nanofluid towards an exponential stretching sheet. BACHOK et al [28] reported the boundary layer flow and heat transfer near a stagnation-point towards an exponentially stretching/shrinking sheet filled with nanofluid. HAYAT et al [29] studied the MHD boundary layer flow of nanofluid past an exponentially stretching sheet in a porous medium in the presence of convective boundary conditions. NADEEM et al [30−31] investigated the MHD three-dimensional boundary layer flow of Casson nanofluid over a linearly stretching sheet with convective boundary condition and they also analyzed the three-dimensional flow of water-based nanofluid over an exponentially stretching sheet. NADEEM et al [32] illustrated the MHD boundary layer flow and the heat transfer of a Maxwell fluid past a stretching sheet in the presence of nanoparticles. Recently, SHEHZAD et al [33] studied two-dimensional boundary layer flow of the third grade nanofluid over a stretching surface with Newtonian heating and viscous dissipation.

The unsteady flow over an exponentially shrinking sheet in the presence of nanoparticles becomes a very important problem when heat transfer is involved in the flow. Hence in the present paper, the unsteady boundary layer flow of nanofluid and heat transfer over an exponentially shrinking porous sheet with suction is investigated. Using suitable transformations, the governing equations are transformed and then those equations are solved numerically using Keller-box method. Then, computed results are plotted in graphs and discussed in detail.

2 Mathematical formulation

Consider the unsteady two-dimensional incompressible fluid over an exponentially shrinking porous sheet filled with a nanofluid containing water based copper in the presence of suction. The governing equations of motion and the energy equation are written as [17, 28]

$$\frac{\partial u}{\partial x}+\frac{\partial v}{\partial y}=0 \tag{1}$$

$$\frac{\partial u}{\partial t}+u\frac{\partial u}{\partial x}+v\frac{\partial u}{\partial y}=\frac{\mu_{\rm nf}}{\rho_{\rm nf}}\frac{\partial^2 u}{\partial y^2} \tag{2}$$

$$\frac{\partial T}{\partial t}+u\frac{\partial T}{\partial x}+v\frac{\partial T}{\partial y}=\alpha_{\rm nf}\frac{\partial^2 T}{\partial y^2} \tag{3}$$

subjected to the boundary conditions

$$\begin{cases} t<0:\ u=0,\ v=0,\ T=T_\infty \ \text{for all}\ x,\ y \\ t\ge 0:\ u=-U_w,\ v=-v_w,\ T=T_w(x,t)=T_\infty+\dfrac{T_0\mathrm{e}^{x/2L}}{(1-\gamma t)} \\ \quad \text{at}\ y=0;\ u\to 0,\ T\to T_\infty,\ \text{as}\ y\to\infty \end{cases} \tag{4}$$

where u and v are the velocity components along x and y directions, respectively; $U_w = a\mathrm{e}^{x/L}/(1-\gamma t)$ is the variable shrinking velocity with a and γ being positive constants with dimensions $\boldsymbol{LT^{-1}}$ and $\boldsymbol{T^{-1}}$, respectively, $v_\mathrm{w} = v_0\mathrm{e}^{x/2L}/\sqrt{1-\gamma t}$ is the variable suction velocity with $v_0>0$ being a constant; T is the temperature of the nanofluid; T_0 is a reference temperature, L is the reference length; μ_nf is the viscosity of the nanofluid; ρ_nf is the density of the nanofluid; α_nf is the thermal diffusivity of the nanofluid, which are defined as (OZTOP and ABU-NADA [34])

$$\alpha_\mathrm{nf} = \frac{k_\mathrm{nf}}{(\rho c_p)_\mathrm{nf}}$$

$$\rho_\mathrm{nf} = (1-\phi)\rho_\mathrm{f} + \phi\rho_\mathrm{s}$$

$$\mu_\mathrm{nf} = \frac{\mu_f}{(1-\phi)^{2.5}}$$

$$(\rho c_p)_\mathrm{nf} = (1-\phi)(\rho c_p)_\mathrm{f} + \phi(\rho c_p)_\mathrm{s}$$

$$\frac{k_\mathrm{nf}}{k_\mathrm{f}} = \frac{(k_\mathrm{s}+2k_\mathrm{f}) - 2\phi(k_\mathrm{f}-k_\mathrm{s})}{(k_\mathrm{s}+2k_\mathrm{f}) + \phi(k_\mathrm{f}-k_\mathrm{s})}$$

where ϕ is the solid volume fraction of the nanofluid; k_nf is the thermal conductivity of the nanofluid; $(\rho c_\mathrm{p})_\mathrm{nf}$ is the heat capacity of the nanofluid; μ_f is the viscosity of the base fluid; k_f is the thermal conductivity of the base fluid; k_s is the thermal conductivity of the solid fractions; $(\rho c_\mathrm{p})_\mathrm{f}$ is the specific heat parameter of the base fluid; $(\rho c_\mathrm{p})_\mathrm{s}$ is the specific heat parameter of the solid fractions. A physical sketch of the flow problem is shown in Fig. 1.

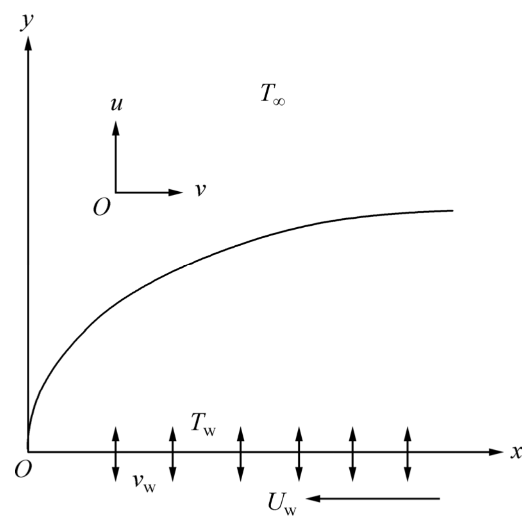

Fig. 1 Physical model and coordinate system

The continuity Eq. (1) is satisfied by introducing a stream function ψ such that

$$u = \frac{\partial \psi}{\partial y}, v = -\frac{\partial \psi}{\partial x}$$

Introducing the following transformations

$$\begin{cases} u = \dfrac{a}{(1-\gamma t)}\mathrm{e}^{x/L} f'(\eta) \\ v = -\sqrt{\dfrac{a\upsilon_f}{2L(1-\gamma t)}}\mathrm{e}^{x/2L}\left[f(\eta) + \eta f'(\eta)\right] \\ \eta = \sqrt{\dfrac{a}{2L\upsilon_f(1-\gamma t)}} e^{x/2L} y \\ \theta(\eta) = \dfrac{T-T_\infty}{T_w - T_\infty} \end{cases} \tag{5}$$

Using Eq. (5), the nonlinear partial differential Eqs. (2) and (3) are transformed into the following ordinary differential equations:

$$\frac{1}{(1-\phi)^{2.5}\left(1-\phi+\phi\dfrac{\rho_\mathrm{s}}{\rho_\mathrm{f}}\right)} f''' + ff'' - 2f'^2 - A(2f' + \eta f'') = 0 \tag{6}$$

$$\frac{k_\mathrm{nf}/k_\mathrm{f}}{1-\phi+\phi\dfrac{(\rho c_p)_\mathrm{s}}{(\rho c_p)_\mathrm{f}}}\theta'' + Prf\theta' - Prf'\theta - APr(2\theta + \eta\theta') = 0 \tag{7}$$

subjected to the transformed boundary conditions:

$$f(0) = S,\ f'(0) = -1,\ \theta(0) = 1, f'(\infty) \to 0,\ \theta(\infty) \to 0 \tag{8}$$

where prime denotes differentiation with respect to η; $Pr=\upsilon_\mathrm{f}/\alpha_\mathrm{f}$ is the Prandtl number; $S = v_0\sqrt{2L/(a\upsilon_\mathrm{f})} > 0$ is the suction parameter; $A=\gamma L\mathrm{e}^{-x/L}/a$ is the unsteady parameter which is x dependent. Therefore, the solution in unsteady flow situation is of non-similar type and the similarity solution exists only when A=0. So, for unsteady flow of nanofluid due to an exponentially shrinking sheet, only non-similar solution is obtained.

Quantities of physical interest are the local skin friction coefficient and the local Nusselt number which are defined as

$$C_\mathrm{f} = \frac{\mu_\mathrm{nf}}{\rho_\mathrm{f} U_\mathrm{w}^2}\left(\frac{\partial u}{\partial y}\right)_{y=0},\ Nu_x = -\frac{xk_\mathrm{nf}}{k_\mathrm{f}(T_\mathrm{w} - T_\infty)}\left(\frac{\partial T}{\partial y}\right)_{y=0} \tag{9}$$

that is,

$$C_\mathrm{f} Re_x^{1/2}\sqrt{\frac{2L}{x}} = \frac{1}{(1-\phi)^{2.5}} f''(0),$$

$$Nu_x Re_x^{-1/2}\sqrt{\frac{2L}{x}} = -\frac{k_\mathrm{nf}}{k_\mathrm{f}}\theta'(0) \tag{10}$$

where $Re_x = xU_\mathrm{w}/\upsilon_\mathrm{f}$ is the local Reynolds number.

3 Numerical method

The transformed Eqs. (6) and (7) subjected to the boundary conditions (Eq. (8)) are solved numerically using the Keller-box method. This method has been found to be very suitable in dealing with nonlinear parabolic problems. By introducing the new dependent variables, these equations are first written as a system of first-order equations which are then expressed in finite difference forms using central differences. Since the system of equations is nonlinear, it is linearized by Newton's method before putting them in matrix-vector form. The resulting linear system is solved along with the boundary conditions by the block-tridiagonal-elimination method. In this study, we used Matlab software. Here, the grid size in η of 0.01 has been used and the convergence criterion was set to 0.5×10^{-5}, which gives accuracy to four decimal places. It should be mentioned that the dual solutions are obtained by setting different values of η_∞ depending on the parameters involved.

4 Results and discussion

The numerical solutions are obtained using the above numerical scheme for some values of the governing parameters, namely, unsteady parameter A, nanoparticle volume fraction parameter ϕ and suction parameter S and non-similar solutions for velocity and temperature are obtained. During the computation, following HAYAT et al [29] and KHANAFER et al [35], the Prandtl number of base fluid is taken as unity and the volume fraction of nanoparticles is taken from 0 to 0.2 ($0\le\phi\le0.2$) in which ϕ=0 corresponds to the viscous or regular fluid. The thermophysical properties of the base fluid and the nanoparticles are listed in Table 1.

Table 1 Thermophysical properties of fluid and nanoparticles

Material	C_p/(J·kg^{-1}·K^{-1})	ρ/(kg·m^{-3})	k/(W·m^{-1}·K^{-1})	α/(10^{-7}m^2·s^{-1})
Fluid phase (water)	4179	997.1	0.613	1.47
Cu	385	8933	400	1163.1

At first, to ensure the numerical accuracy, the dual velocity profiles are compared with the results obtained by BHATTACHARYYA [12] in Fig. 2 for A=0, ϕ=0, S=2.4. Those are found in excellent agreements.

The variations of $f''(0)$ and $-\theta'(0)$ which are related to local skin friction coefficient and local Nusselt number respectively, with suction parameter S for different values of A and ϕ are shown in Figs. 3−6. It is observed that the dual non-similar solutions (similarity solution for steady case) are obtained for $S\ge S_c$ and the flow has no solution for $S<S_c$ where S_c is the critical value of S. Based on our calculation, the critical values are 1.9300, 1.9079 and 1.8755 for A=0, A=0.1 and A=0.2, respectively, when ϕ=0. While the critical values for ϕ=0, 0.1, 0.2 are 2.2338, 1.9079 and 1.8500, respectively, when A=0.1. Hence, the unsteady parameter A and nanoparticle volume fraction parameter ϕ widen the range of mass suction parameter S for which the non-

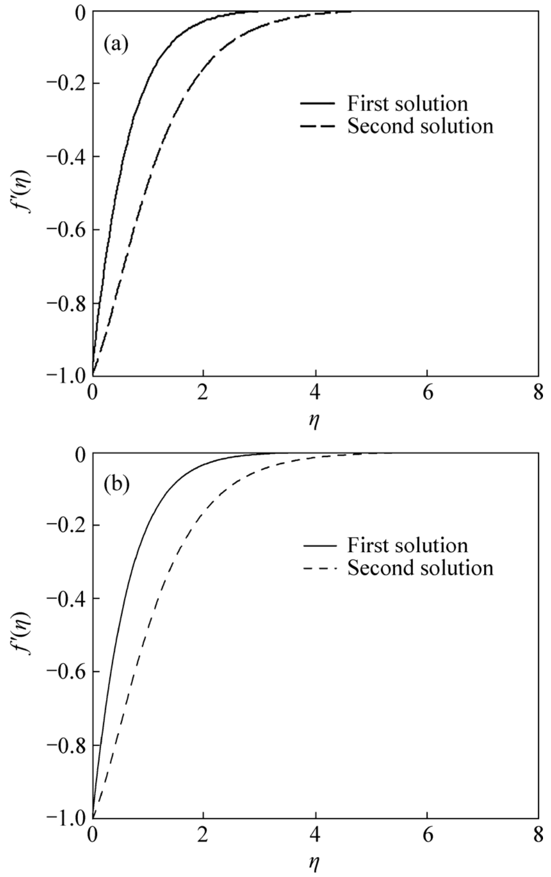

Fig. 2 Comparison of velocity profiles for A=0, ϕ=0, S=2.4 in present study (a) and Ref. [12] (b)

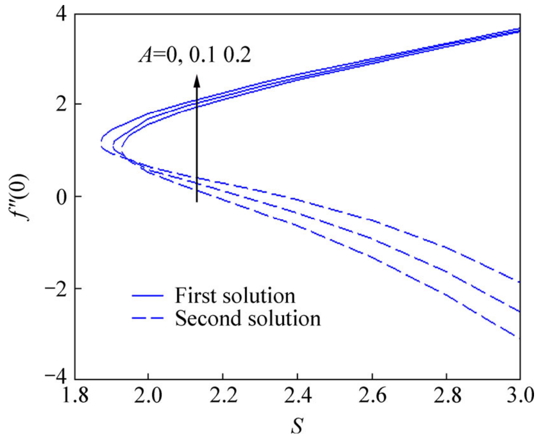

Fig. 3 Variation of $f''(0)$ with S for different values of A with ϕ=0.1

similar solution exists. It is also observed from the figures that the value of $f''(0)$ increases for the first and second solutions, while it increases for fist solution and decreases for the second solution with increasing values of S and ϕ. On the other hand, the value of $-\theta'(0)$ and consequently the rate of heat transfer enhance with A and ϕ for both solution branches.

The boundary layer velocity and temperature profiles for various values of nanoparticle volume fraction parameter ϕ are plotted in Figs. 7 and 8. The

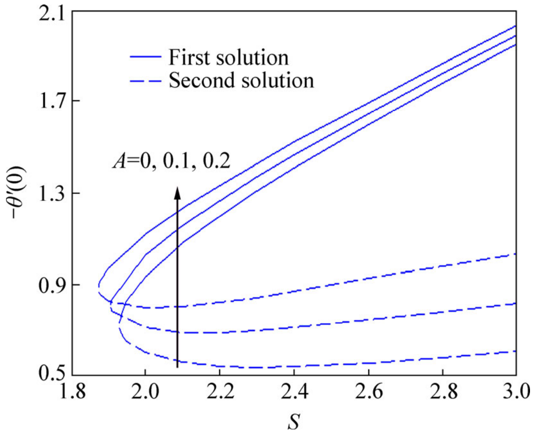

Fig. 4 Variation of $-\theta'(0)$ with S for different values of A with ϕ=0.1

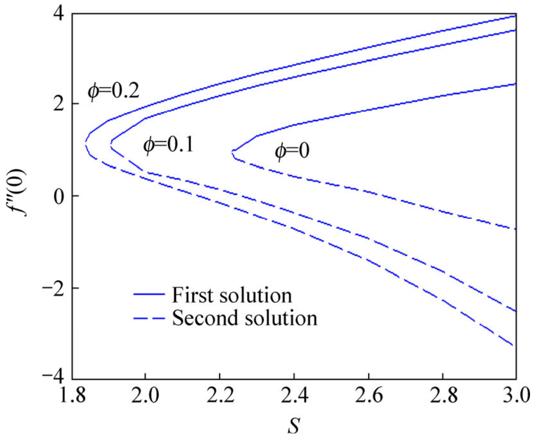

Fig. 5 Variation of $f''(0)$ with S for different values of ϕ with A=0.1

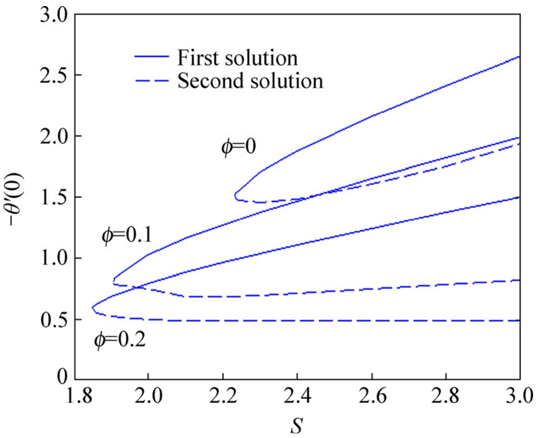

Fig. 6 Variation of $-\theta'(0)$ with S for different values of ϕ with A=0.1

profiles of velocity demonstrate conflicting character for first and second solutions. Figure 7 shows that the velocity of the fluid increases with ϕ for the first solution. This is due to the fact that when the volume of copper nanoparticles increases, the thermal conductivity increases and hence the boundary layer thickness decreases. Whereas, the opposite effect is observed in the case of the second solution. Figure 8 illustrates that the

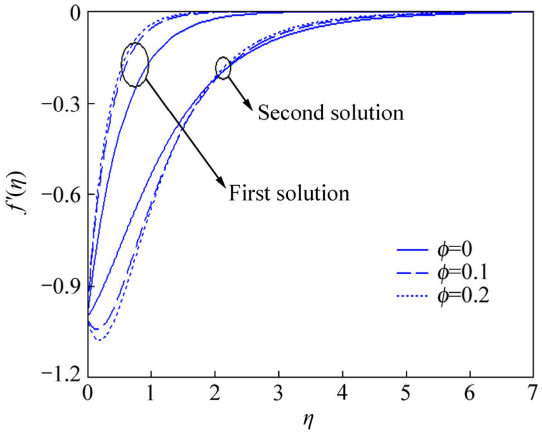

Fig. 7 Velocity profiles for different values of ϕ with A=0.1 and S=2.4

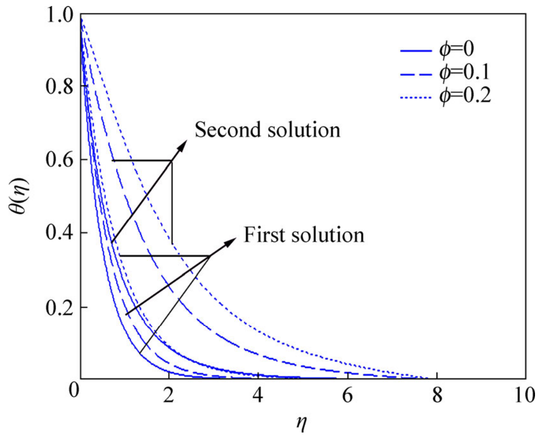

Fig. 8 Temperature profiles for different values of ϕ with A=0.1 and S=2.4

temperature of fluid increases with increasing ϕ for the first and second solutions and consequently the thickness of thermal boundary layer increases.

Figures 9 and 10 display the velocity and temperature profile for various suction parameter S. From Fig. 9, it is observed that the velocity boundary layer thickness decreases with increasing suction for the first solution, while the opposite effect is observed in the

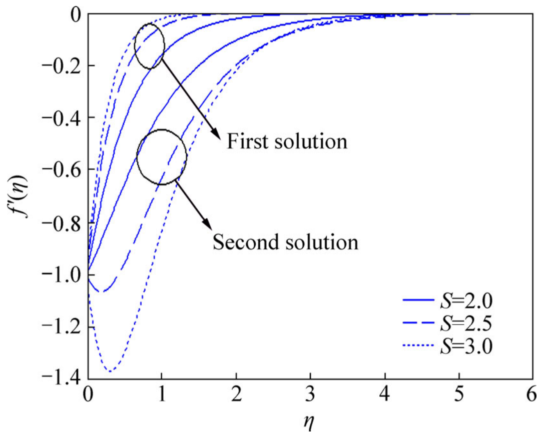

Fig. 9 Velocity profiles for different values of S with A=0.05 and ϕ=0.1

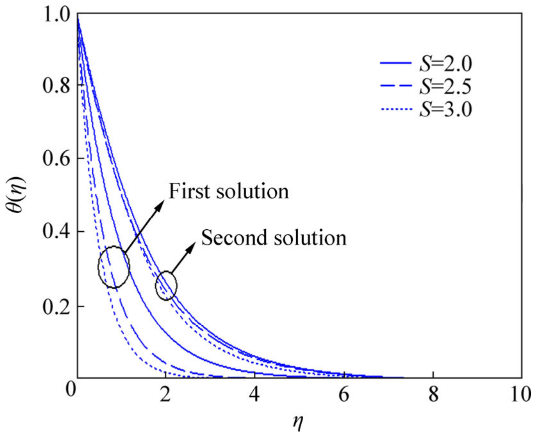

Fig. 10 Temperature profiles for different values of S with A=0.05 and ϕ=0.1

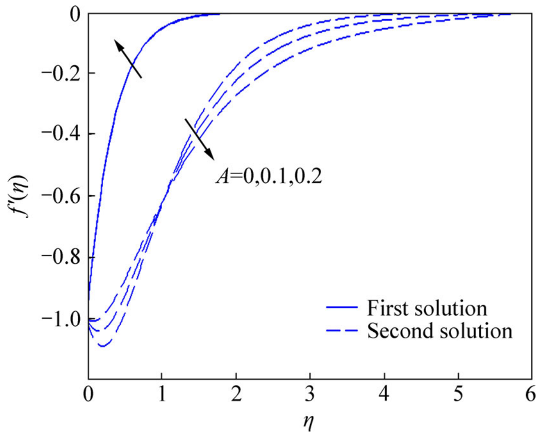

Fig. 11 Velocity profiles for different values of A with ϕ=0.1 and S=2.5

case of the second solution. Figure 10 shows that the temperature of fluid decreases with increasing suction for the fist and second solutions and consequently, the thermal boundary layer thickness decreases for both solutions.

The effect of unsteady parameter A on the velocity and temperature profiles is illustrated in Figs. 11 and 12. The effect of unsteady parameter A is major in the second solution branch. From Fig. 11, it is observed that the velocity boundary layer thickness slightly decreases with increasing unsteady parameter in the first solution, while the opposite effect is observed in the second solution. Figure 12 shows that the temperature of fluid decreases with increasing of unsteady parameter in the case of both solutions near the sheet, but reverse effect away from the sheet. Consequently, the thickness of thermal boundary layer increases.

It is also interesting to note that similar to steady flow case the velocity and thermal boundary layer thicknesses for the second solution are always thicker than those of the first solution. Also, all obtained results of velocity and temperature satisfy the far field boundary

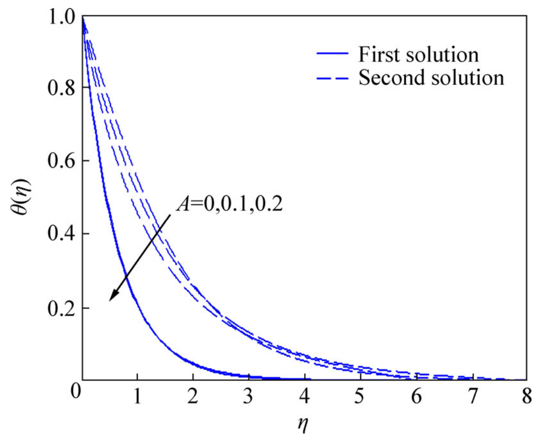

Fig. 12 Temperature profiles for different values of A with ϕ=0.1 and S=2.5

conditions asymptotically, which strongly indicates that the computed numerical results are true. In addition, grid independence test has been carried out and the values of $f''(\eta)$ and $\theta(\eta)$ for A=0.1, ϕ=0.1, S=2.5 by taking the grid sizes as 0.005, 0.01, 0.015 are presented in Table 2, which shows the results in good agreement.

Table 2 Grid sensitivity analysis with A=0.1, ϕ=0.1, S=2.5

Function	Solution	h	η						
			0.5	1	2	3	4	6	8
$f'(\eta)$	First solution	0.005	−0.2394	−0.0565	−0.0034	−0.0002	0.0000	0.0000	
		0.01	−0.2400	−0.0567	−0.0036	−0.0003	0.0000	0.0000	
		0.015	−0.2410	−0.0573	−0.0039	−0.0006	0.0000	0.0000	
	Second solution	0.005	−0.9312	−0.6331	−0.2257	−0.0770	−0.0279	−0.0044	0.0000
		0.01	−0.9310	−0.6330	−0.2256	−0.0769	−0.0278	−0.0043	0.0000
		0.015	−0.9305	−0.6325	−0.2251	−0.0762	−0.0274	−0.0038	0.0000
$\theta(\eta)$	First solution	0.005	0.4538	0.2066	0.0451	0.0103	0.0024	0.0000	
		0.01	0.4545	0.2071	0.0455	0.0105	0.0025	0.0000	
		0.015	0.4550	0.2077	0.0457	0.0108	0.0026	0.0000	
	Second solution	0.005	0.7159	0.5112	0.2571	0.1314	0.0690	0.0188	0.0000
		0.01	0.7158	0.5111	0.2570	0.1313	0.0689	0.0187	0.0000
		0.015	0.7150	0.5003	0.2561	0.1304	0.0680	0.0179	0.0000

5 Conclusions

From the study following remark can be concluded.

1) Dual non-similar solutions are obtained in certain range of the suction parameter.

2) It is important to note that due to unsteadiness of the flow and the presence of nanoparticles in the flow field the requirement of mass suction for the existence of non-similar solution becomes less, namely, for weaker mass suction the solutions exist.

3) The velocity of fluid increases for the first solution and decreases for the second solution with increasing nanoparticle volume fraction, while, the temperature of fluid increases with nanoparticle volume fraction for both solutions.

4) Due to increase in suction parameter, the velocity boundary layer thickness decreases for the first solution and increases in case of the second solution. On the other hand, the thermal boundary layer thickness decreases for both solutions. Whereas, the velocity of fluid increases in the first solution and decreases in the second solution and the temperature of fluid decreases for both solutions.

5) Due to the unsteadiness of the flow, the temperature inside the boundary layer decreases for both solutions near the sheet.

6) And most importantly, for the presence of unsteadiness and the nanoparticles in the flow, the boundary layer separation is slightly delayed.

Acknowledgements

Authors are thankful to the reviewers for their constructive comments and suggestions which led to definite improvement of the paper. One of the authors, K. Bhattacharyya is grateful to the National Board for Higher Mathematics (NBHM), Department of Atomic Energy, Government of India for the financial support in pursuing this work. Also, S. Shafie acknowledges the financial support from MOHE and the Research Management Center-UTM through FRGS and RUG vote number 4F109 and 02H80 for this research.

Nomenclature

A	Unsteadiness parameter
L	Reference length
S	Suction parameter
f	Dimensionless stream function
C_f	Skin friction coefficient
C_p	Specific heat capacity at constant pressure
k	Thermal conductivity
Nu_x	Local Nusselt number
Pr	Prandtl number
Re_x	Local Reynolds number
t	Time
v_w	Suction velocity
T	Fluid temperature
T_w	Surface temperature
U_w	Shrinking velocity
T_∞	Ambient temperature
u,v	Velocity components along x- and y- direction, respectively.
x,y	Cartesian coordinate along surface and normal to it, respectively.

Greek symbols

α	Thermal diffusivity
η	Similarity variables
μ	Dynamic viscosity
υ	Kinematic viscosity
ϕ	Nanoparticle volume fraction
ρ	Fluid density
ψ	Stream function
θ	Dimensionless temperature

Subscripts

f	Fluid
s	Solid
nf	Nanofluid
w	Condition at surface
∞	Ambient condition

Superscript

′	Differentiation with respect to η

References

[1] CRANE L J. Flow past a stretching plate [J]. ZAMP, 1970, 21: 645−647.

[2] WANG C Y. Liquid film on an unsteady stretching sheet [J]. Q Appl Math, 1990, 48: 601−610.

[3] MIKLAVČIČ M, WANG C Y. Viscous flow due a shrinking sheet [J]. Q Appl Math, 2006, 64: 283−290.

[4] WANG C Y. Stagnation flow towards a shrinking sheet [J]. Int J Nonlinear Mech, 2008, 43: 377−382.

[5] FANG T. Boundary layer flow over a shrinking sheet with power-law velocity [J]. Int J Heat Mass Transfer, 2008, 51: 5838−5843.

[6] BHATTACHARYYA K. Effects of heat source/sink on MHD flow and heat transfer over a shrinking sheet with mass suction [J]. Chem Eng Res Bull, 2011, 15: 12−17.

[7] HAYAT T, HUSSAIN M, HENDI A A, NADEEM S. MHD stagnation point flow towards a heated shrinking surface subjected to heat generation/absorption [J]. Appl Math Mech: Engl Edit, 2012, 33(5): 631−648.

[8] BHATTACHARYYA K, ARIF M G, ALI PK W. MHD boundary layer stagnation-point flow and mass transfer over a permeable shrinking sheet with suction/blowing and chemical reaction [J]. Acta Technica, 2012, 57: 1−15.

[9] BHATTACHARYYA K. Heat transfer in boundary layer stagnation-point flow towards a shrinking sheet with non-uniform heat flux [J]. Chin Phys B, 2013, 22(7): 074705.

[10] MIDYA C. Heat transfer in MHD boundary layer flow over a shrinking sheet with radiation and heat sink [J]. J Global Res Math Arch, 2013, 1(2): 63−70.

[11] MAGYARI E, KELLER B. Heat and mass transfer in the boundary layers on an exponentially stretching continuous surface [J]. J Phys D

Appl Phys, 1999, 32: 577−585.

[12] BHATTACHARYYA K. Boundary layer flow and heat transfer over an exponentially shrinking sheet [J]. Chin Phy Lett, 2011, 28: 074701.

[13] BHATTACHARYYA K, POP I. MHD boundary layer flow due to an exponentially shrinking sheet [J]. Magnetohydrodynamics, 2011, 47: 337−344.

[14] BHATTACHARYYA K, VAJRAVELU K. Stagnation-point flow and heat transfer over an exponentially shrinking sheet [J]. Communications in Nonlinear Science and Numerical Simulation, 2012, 17: 2728−2734.

[15] FANG T G, ZHANG J, YAO S S. Viscous flow over an unsteady shrinking sheet with mass transfer [J]. Chin Phys Lett, 2009, 26: 014703.

[16] CORTELL R. On a certain boundary value problem arising in shrinking sheet flows [J]. Appl Math Comput, 2010, 217: 4086−4093.

[17] BHATTACHARYYA K. Heat transfer analysis in unsteady boundary layer stagnation-point flow towards a shrinking/stretching sheet [J]. Ain Shams Eng J, 2013, 4: 259−264.

[18] CHOI S U S. Enhancing thermal conductivity of fluids with nanoparticles [C]// The Proceedings of the 1995 ASME International Mechanical Engineering Congress and Exposition. San Francisco, USA: ASME, FED 231/MD, 1995, 66: 99−105.

[19] BUONGIORNO J. Convective transport in nanofluids [J]. ASME J Heat Transfer, 2006, 128: 240−250.

[20] WONG K V, LEON O D. Applications of nanofluids: Current and future [J]. Adv Mech Eng, 2010, 2010: 519659.

[21] DAS, S K, CHOI S U S, YU, W, PRADEEP T. Nanofluids: Science and technology [M]. Hoboken, NJ, USA: John Wiley & Sons, 2007.

[22] SAIDUR R, LEONG K Y, MOHAMMAD H A. A review on applications and challenges of nanofluids [J]. Renewable and Sustainable Energy Reviews, 2011, 15(3): 1646−1668.

[23] MAKINDE O D, AZIZ A. Boundary layer flow of a nanofluid past a stretching sheet with a convective boundary condition [J]. Int J Thermal Sci, 2011, 50: 1326−1332.

[24] MUSTAFA M, HAYAT T, POP I, ASGHAR S, OBAIDAT S. Stagnation point flow of nanofluid over a stretching sheet [J]. Int J Heat Mass Transfer, 2011, 54: 5588−5594.

[25] RANA P, BHARGAVA R. Flow and heat transfer of a nanofluid over a nonlinearly stretching sheet: A numerical study [J]. Common Nonlinear Sci Num Simul, 2012, 17: 212−226.

[26] HADY F M, IBRAHIM F S, ABDEL-GAIED S M, EID M R. Radiation effect on viscous flow of a nanofluid and heat transfer over a nonlinearly stretching sheet [J]. Nanoscale Res Lett, 2012, 7: 229.

[27] NADEEM S, LEE C. Boundary layer flow of nanofluid over an exponentially stretching surface [J]. Nanoscale Res Lett, 2012, 7: 94.

[28] BACHOK N, ISHAK A, POP I. Boundary layer stagnation-point flow and heat transfer over an exponentially stretching/shrinking sheet in a nanofluid [J]. Int J Heat Mass Transfer, 2012, 55: 8122−8128.

[29] HAYAT T, IMTIAZA M, ALSAEDI A, MANSOOR R. MHD flow of nanofluids over an exponentially stretching sheet in a porous medium with convective boundary conditions [J]. Chin Phys B, 2014, 23: 054701.

[30] NADEEM S, HAQ R U, AKBAR N S. MHD three-dimensional boundary layer flow of Casson nanofluid past a linearly stretching sheet with convective boundary condition [J]. IEEE Trans Nanotechnology, 2014, 13: 109−115.

[31] NADEEM S, HAQ R U, KHAN Z H. Heat transfer analysis of water-based nanofluid over an exponentially stretching sheet [J]. Alexandria Eng J, 2014, 53: 219−224.

[32] NADEEM S, HAQ R U, KHAN Z H. Numerical study of MHD boundary layer flow of a Maxwell fluid past a stretching sheet in the presence of nanoparticles [J]. Journal of the Taiwan Institute of Chemical Engineers, 2014, 45: 121−126.

[33] SHEHZAD S A, HUSSAIN T, HAYAT T, RAMZAN M, ALSAEDI A. Boundary layer flow of third grade nanofluid with Newtonian heating and viscous dissipation [J]. Journal of Central South University, 2015, 22(1): 360−367.

[34] OZTOP H F, ABU-NADA E. Numerical study of natural convection in partially heated rectangular enclosures filled with nanofluids [J]. Int J Heat Fluid Flow, 2008, 29: 1326−1336.

[35] KHANAFER K, VAFAI K, LIGHTSTONE M. Buoyancy-driven heat transfer enhancement in a two-dimensional enclosure utilizing nanofluids [J]. Int J Heat Mass Transfer, 2003, 46: 3639−3653.

(Edited by YANG Hua)